JBC RESEARCH ARTICLE

Palmitoylation of the small GTPase Cdc42 by DHHC5 modulates spine formation and gene transcription

Received for publication, April 8, 2022, and in revised form, May 11, 2022 Published, Papers in Press, May 18, 2022,
https://doi.org/10.1016/j.jbc.2022.102048

Alexander Wirth[1], Josephine Labus[1], Dalia Abdel Galil[1], Yvonne Schill[1], Silke Schmidt[1], Tania Bunke[1], Nataliya Gorinski[1], Norihiko Yokoi[2], Masaki Fukata[2], and Evgeni Ponimaskin[1,*]

From the [1]Cellular Neurophysiology, Hannover Medical School, Hannover, Germany; [2]Division of Membrane Physiology, Department of Molecular and Cellular Physiology, National Institute for Physiological Sciences, National Institutes of Natural Sciences, Okazaki, Japan

Edited by Henrik Dohlman

The small GTPase Cdc42 exists in the form of two alternatively spliced variants that are modified by hydrophobic chains: the ubiquitously expressed Cdc42-prenyl and a brain-specific isoform that can be palmitoylated, Cdc42-palm. Our previous work demonstrated that Cdc42-palm can be palmitoylated at two cysteine residues, Cys188 and Cys189, while Cys188 can also be prenylated. We showed that palmitoylation of Cys188 is essential for the plasma membrane localization of Cdc42-palm and is critically involved in Cdc42-mediated regulation of gene transcription and neuronal morphology. However, the abundance and regulation of this modification was not investigated. In the present study, we found that only a minor fraction of Cdc42 undergoes monopalmitoylation in neuroblastoma cells and in hippocampal neurons. In addition, we identified DHHC5 as one of the major palmitoyl acyltransferases that could physically interact with Cdc42-palm. We demonstrate that overexpression of dominant negative DHHC5 mutant decreased palmitoylation and plasma membrane localization of Cdc42-palm. In addition, knockdown of DHHC5 significantly reduced Cdc42-palm palmitoylation, leading to a decrease of Cdc42-mediated gene transcription and spine formation in hippocampal neurons. We also found that the expression of DHHC5 in the brain is developmentally regulated. Taken together, these findings suggest that DHHC5-mediated palmitoylation of Cdc42 represents an important mechanism for the regulation of Cdc42 functions in hippocampus.

Protein S-palmitoylation (further referred to as palmitoylation) is the reversible modification of cysteine residue(s) within the target proteins *via* thioester bond by the C16 saturated fatty acid palmitate. Palmitoylation has been shown to regulate multiple protein functions, including altering membrane association of peripheral membrane proteins by increasing the hydrophobicity, membrane subdomain compartmentalization, modulating protein–protein interaction, tilting transmembrane domains, and influencing protein stability (1). Since palmitoylation is the only reversible lipid modification, it has been suggested to act as an activity switch for some proteins. For example, activation of sodium channels as well as the activity of sodium calcium exchanger NCX1 is regulated by dynamic palmitoylation (2). Some investigations also demonstrated a pivotal role for the dynamic palmitoylation in neurons. We have shown that postsynaptic density 95 protein (PSD-95) gets palmitoylated close to the plasma membrane and thus promoting its plasma membrane localization, which is essential for its clustering leading to proper synaptic transmission by affecting α-amino-3-hydroxy-5-methyl-4-isoxazolepropionic acid receptor functions (3). Our more recent data revealed that defined members of ABHD serine hydrolases, a new class of depalmitoylation enzymes, might selectively depalmitoylate PSD-95 in neurons making it available for the next palmitoylation cycle (4). In addition, dynamic palmitoylation was suggested to maintain the proper localization and function of the small GTPase H-Ras in living cells (5).

Another well-studied small GTPase undergoing palmitoylation is Cdc42. It is expressed as two isoforms, for which production is regulated by splicing factors polypyrimidine tract-binding protein 1 and 2 (6). Recent research revealed a polarized localization and different functions for both isoforms: The canonical Cdc42 isoform, which is expressed in many tissues, is prenylated, whereas the brain-specific Cdc42 isoform can be palmitoylated. In the brain, the canonical isoform Cdc42-prenyl (also called Cdc42 or Cdc42E7) is primarily located in the axonal compartment. An enrichment of Cdc42-prenyl in axons can be explained by selective axonal translation of Cdc42-prenyl mRNA isoform, which further increases *in vivo* during axon regeneration (7). In contrast, the Cdc42-palm (also called bCdc42 or Cdc42E6) is mainly expressed in dendritic compartments, where it is involved in the activation of gene transcription, regulation of dendrite length, induction of dendritic protrusion, spinogenesis, and modulation of spine morphology (6, 8–10). Moreover, we have recently unraveled a role for Cdc42-palm in long-term spine stabilization and showed that overexpression of a constitutively active form of Cdc42-palm is sufficient to rescue spine stabilization to normal levels in a mouse model of 22q11.2

* For correspondence: Evgeni Ponimaskin, Ponimaskin.Evgeni@mh-hannover.de.

deletion syndrome (11). The Cdc42-palm isoform can be palmitoylated at two cysteine residues, Cys188 and Cys189, even though Cys188 can also be isoprenylated (10).

In the present study, we identified DHHC5 as the palmitoylating enzyme, which preferentially modifies Cys188 within Cdc42-palm. We also demonstrated that shRNA-mediated knockdown of DHHC5 expression leads to decreased Cdc42 palmitoylation resulting in an attenuated Cdc42-mediated transcriptional activation and reduced spine density in hippocampal neurons.

Results

DHHC5 is a major Cdc42 palmitoyl transferase

To identify the enzyme(s) palmitoylating Cdc42, we cotransfected each of the 23 hemagglutinin (HA)-tagged mouse DHHC acyl-transferases together with GFP-tagged Cdc42-palm WT in N1E-115 neuroblastoma cells. Using click chemistry to monitor dynamic palmitoylation levels, we observed substantially increased Cdc42 palmitoylation after coexpression of DHHC5, DHHC10, and DHHC17 (Fig. S1*A*). The more prominent increase in palmitoylation was obtained after coexpression of Cdc42-palm with DHHC5 (Fig. S1*B*), suggesting that DHHC5 belongs to the most potent palmitoyl acyltransferases (PATs) for Cdc42. Since DHHC5 was described to play an important role in processes related to spinogenesis (12, 13), in which Cdc42 is also involved (8, 10), we decided to focus on this particular PAT. Moreover, in contrast to Golgi-resided DHHC10 and DHHC17, DHHC5 is localized at the plasma membrane (14). In accordance with that, the functionality of the Cdc42 also depends on its correct localization at the plasma membrane. Furthermore, Cdc42 was among proteins significantly enriched in the DHHC5 pull-down fraction from the HeLa cell lysates (15).

To further verify the role of DHHC5 as Cdc42 PAT, we coexpressed GFP-tagged Cdc42-palm WT (GFP-Cdc42 palm WT) together with either the WT DHHC5 or its dominant-negative mutant DHHS5, which is not able to transfer palmitate to its substrate (13). As shown in Figure 1, *A* and *B*, expression of the WT DHHC5 led to a significant increase, while overexpression of the dominant-negative DHHS5 mutant to a reduction of the Cdc42 palmitoylation. Of note, coexpression of DHHC5 together with Cdc42-prenyl demonstrated that DHHC5 is not able to palmitoylate this Cdc42 isoform. It is also noteworthy that overexpression of DHHC5 did not alter global palmitoylation level in N1E-115 cells compared to plasmid cloning DNA (pcDNA)–transfected cells (Fig. 1, *C* and *D*).

The role of DHHC5 was further confirmed by a modified acyl-biotinyl exchange approach after either knockdown or overexpression of DHHC5. To silence DHHC5 expression, we developed specific shRNAs. Real-time PCR and Western blot analysis revealed that transfection of N1E cells with corresponding shRNAs significantly decreases the expression of the recombinant HA-DHHC5 as well as mRNA levels of endogenous DHHC5 in case of shRNA #1, which was used for further experiments (Fig. 2, *A*–*C*). More importantly, shRNA-evoked silencing of endogenous DHHC5 decreased the palmitoylation of Cdc42 to 47 ± 21% (p = 0.03) as compared to shRNA-scramble (Fig. 2, *D* and *E*). In contrast, overexpression of DHHC5 significantly increased Cdc42 palmitoylation to 169 ± 44% (p = 0.02; Figure 2, *D* and *E*). Noteworthy, neither overexpression nor shRNA-mediated knockdown of DHHC5 affected expression levels of Cdc42 (Fig. S2*A*). As additional control for DHHC5 specificity, we analyzed Cdc42 palmitoylation after knockdown of nonrelevant DHHC6 using specific shRNA (Fig. S2, *B*–*D*). These experiments revealed that knockdown of DHHC6 does not affect Cdc42 palmitoylation level (Fig. 2, *D* and *E*).

Although the brain-specific Cdc42-palm isoforms possesses two putative palmitoylation sites, its palmitoylation stoichiometry remain elusive. To address this question, we applied acyl-PEGyl exchange gel shift (APEGS) assays developed in our laboratory (4). This assay is based on the labeling of cysteinyl thiols with maleimide-PEG (here with maleimide-PEG-2k), which causes a mobility shift of palmitoylated proteins in SDS-PAGE. Using the APEGS approach, we found that a minor fraction of HA-tagged Cdc42-palm expressed in N1E-115 cells shows a shift of around 2 kDa, pointing to the palmitoylation of only one cysteine residue. Overexpression of DHHC5 increases the relative amount of Cdc42 palmitoylation, although the Cdc42 still remains monopalmitoylated (Fig. 2*F*). We then investigated the palmitoylation stoichiometry of neuronal Cdc42 isoform under endogenous conditions. To this end, we analyzed primary cultures of rat hippocampal neurons at day *in vitro* (DIV) 23, when well-defined synapses are already formed. Using the APEGS assay, we found that under the basal condition, a relatively small fraction of Cdc42-palm isoform exists in a palmitoylated form. However, since anti-Cdc42 antibody used in this study recognizes both Cdc42 isoforms, the stoichiometry might be underestimated. Similar to the recombinant Cdc42 expressed in N1E-115 cells, we obtained only a single shifted band in APEGS experiments demonstrating that also in hippocampal neurons Cdc42 undergoes palmitoylation at a single site (Fig. 2*G*). These results further confirm DHHC5 as a specific Cdc42 palmitoyltransferase and suggest that Cdc42 is preferentially palmitoylated only at one cysteine residue.

DHHC5 interacts with Cdc42 at the plasma membrane

Plasma membrane localization is essential for proper Cdc42-palm functions. We have previously demonstrated a pivotal role of Cys188 lipidation for membrane anchoring of Cdc42 (10). Having shown that DHHC5 is a Cdc42 PAT, we verified a possible role of this enzyme for subcellular Cdc42 distribution. After coexpression of GFP-tagged DHHC5 with mCherry-tagged Cdc42-palm, we obtained a high degree of colocalization of both proteins at the plasma membrane (Fig. 3*A*). Similar overlapping distributions were also obtained after coexpression of DHHC5 and Cdc42-palm mutant C189A. In contrast, mutation of Cys188, either alone or in combination with Cys189, results in diffuse cytosolic and nuclear Cdc42 distribution, leading to a drastic decrease of the membrane colocalization with DHHC5 (Fig. 3*A*).

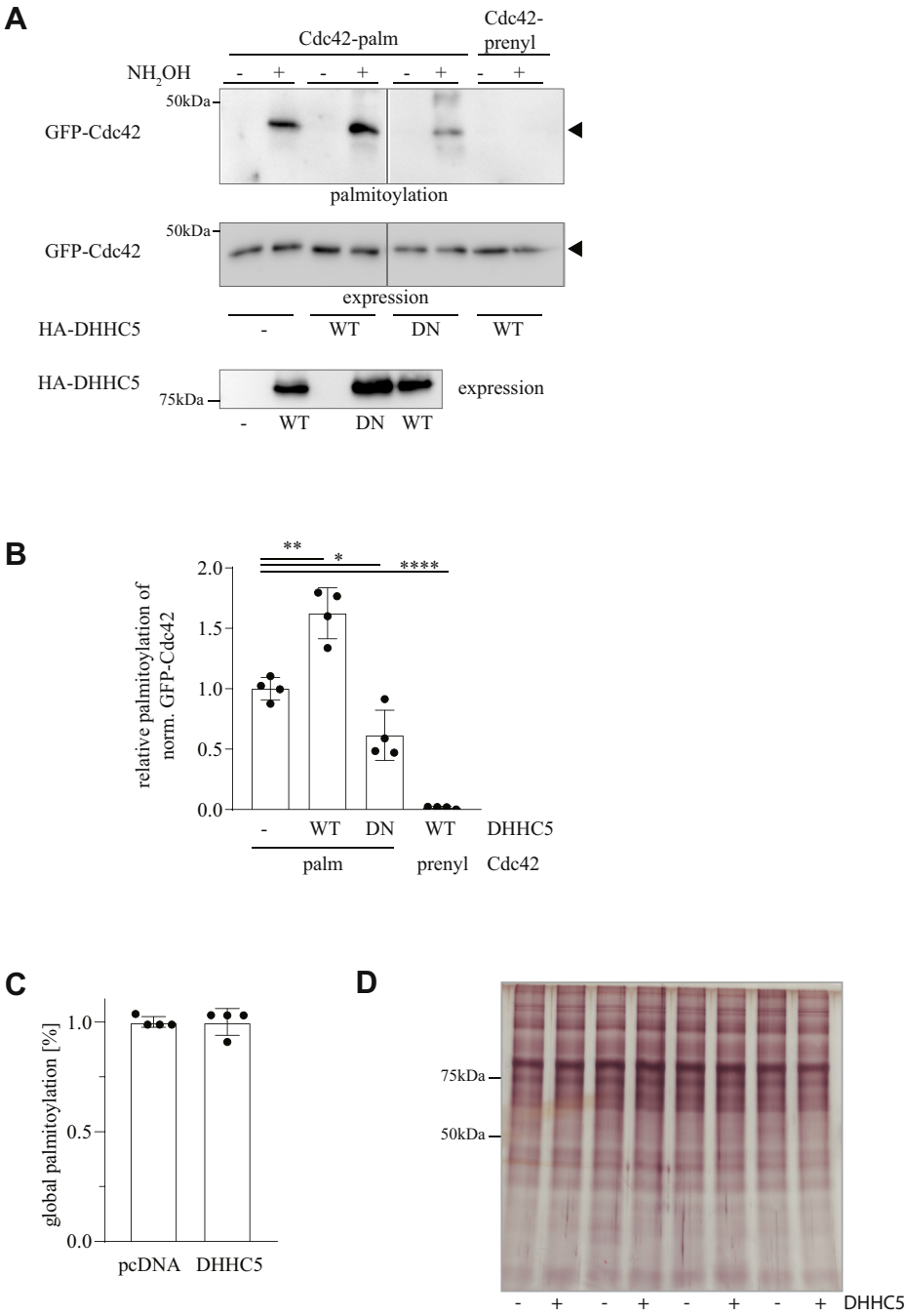

Figure 1. DHHC5 is a putative palmitoyl acyltransferase for Cdc42-palm. *A*, representative Western blots of ABE experiments to validate palmitoylation of Cdc42 after overexpression of either WT or dominant-negative (DN) mutant of HA-tagged DHHC5. The *upper panel* represents the palmitoylation of Cdc42-palm; *middle panel* shows the expression of GFP-tagged Cdc42. In both cases, anti-GFP antibody was used for detection. The *lowest panel* shows expression of HA-tagged DHHC5 protein (detected with anti-HA antibody). *B*, quantification of the relative palmitoylation level of GFP-tagged Cdc42 in the presence of DHHC5 WT or its DN mutant. N = 4, one-way ANOVA with Holm–Sidak's multiple comparisons tests. *$p < 0.05$, **$p < 0.01$, ***$p < 0.0001$. *C*, analysis of the global palmitoylation levels assessed after quantification of the silver staining gels (*D*) after ABE. ABE, acyl-biotinyl exchange; HA, hemagglutinin.

Noteworthy, when WT Cdc42-palm was coexpressed with the dominant negative DHHS5 mutant (which was still resided at the plasma membrane), the plasma membrane localization of Cdc42 was significantly decreased to the level obtained for palmitoylation-deficient Cdc42 mutants (Fig. 3, *A* and *B*). Detailed quantitative analyses of the distribution of mCherry-tagged Cdc42-palm revealed a significant reduced fraction of the Cys188 mutant as well as the double mutant of Cdc42-palm resided at the plasma membrane (Fig. 3*B*). Interestingly, the coexpression of mCherry-tagged Cdc42-palm WT with the dominant negative DHHC5 mutant results in significant lower plasma membrane appearance of Cdc42-palm. (Fig. 3*B*). Of note, the DHHC5 overexpression seems to be not necessary for the correct localization of Cdc42-palm at

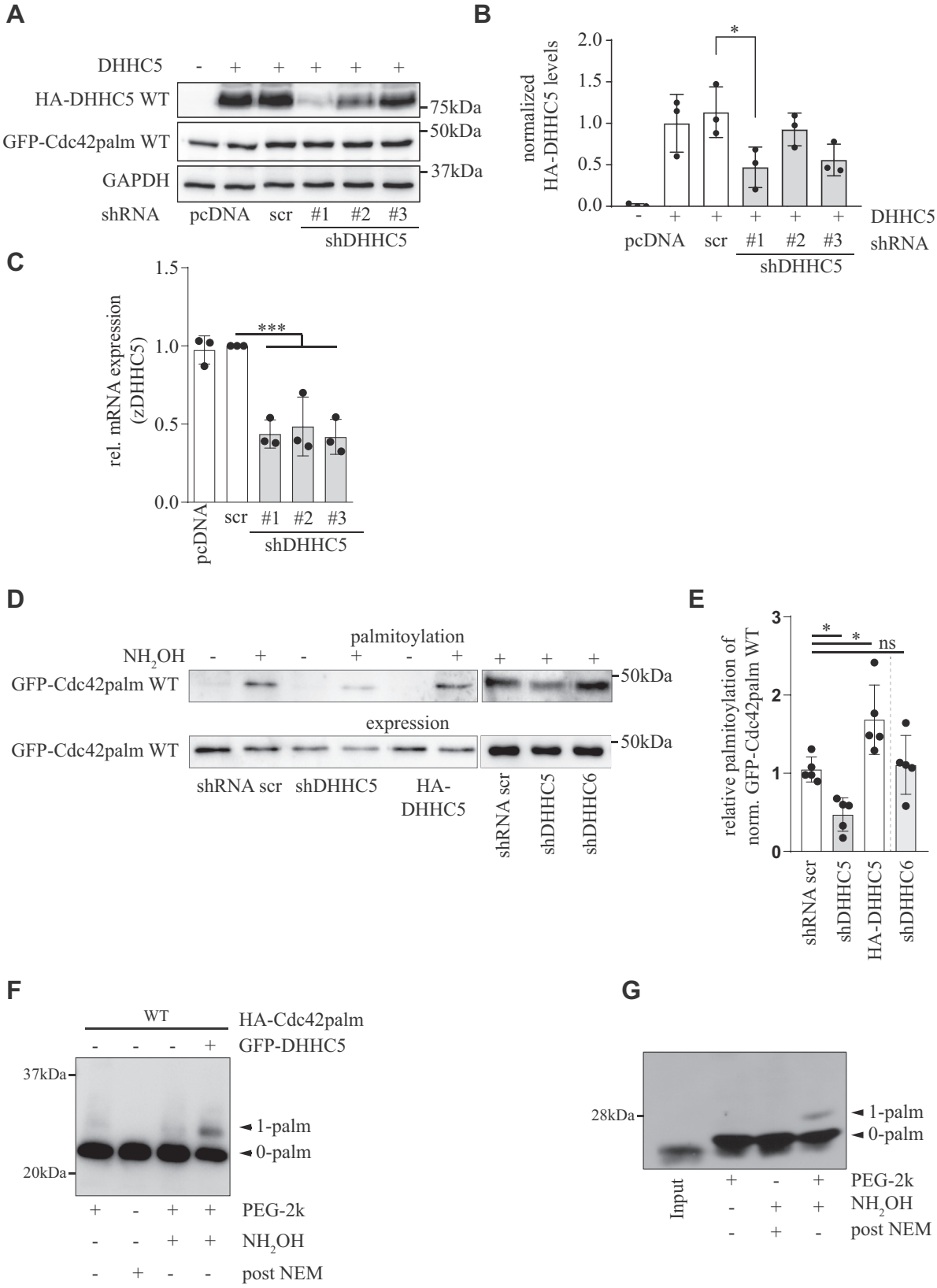

Figure 2. Verification of DHHC5 specificity toward Cdc42 palmitoylation. *A*, validation of shRNAs to knockdown expression of exogenous HA-tagged DHHC5 in N1E-115 cells (*upper panel*). *Middle panel* shows expression of Cdc42-palm and *lower panel*—expression of GAPDH. Cells transiently transfected with scrambled (scr) shRNA or pcDNA were used as a control. Representative Western blots are shown. *B*, quantification of the normalized protein levels of HA-tagged DHHC5 under indicated conditions. N = 3, one-way ANOVA with Tukey's multiple comparison test. *$p < 0.05$. *C*, relative amount of the mRNA encoding endogenous DHHC5 in N1E-115 cells expressing indicated shRNAs was analyzed by qRT-PCR (N = 3). one-way ANOVA with Dunnetts' multiple comparison, ***$p < 0.001$. *D*, representative images of the ABE assay followed by SDS-PAGE and Western blot on GFP-tagged Cdc42-palm coexpressed in

the plasma membrane because the recombinant WT Cdc42 still resides at the plasma membrane when expressed alone (10).

These data suggest that DHHC5 regulates Cdc42 localization at the plasma membrane in dependence on its enzymatic activity. One possible underlying mechanism might involve physical interaction (either direct or mediated by the other proteins) between Cdc42 and DHHC5. To proof for that, we applied coimmunoprecipitation (co-IP) experiments in N1E-115 cells transiently coexpressing HA-tagged DHHC5 and GFP-tagged Cdc42. Figure 3*C* shows that after immunoprecipitation with an antibody against the GFP-tag, the HA-tagged DHHC5 was identified mainly in samples derived from cells coexpressing both Cdc42 WT and DHHC5. Similar results were obtained after coexpression of DHHC5 with the Cys189 Cdc42 mutant. It is noteworthy that specific interaction was diminished when Cys188 or Cys188/Cys189 Cdc42-palm mutants were coexpressed with DHHC5, suggesting a critical role of Cys188 as palmitoyl acceptor for the interaction (Fig. 3*C*). Specific interaction between DHHC5 and Cdc42-palm was further supported by the observation that the coexpression of DHHC5 with GFP-tagged Cdc42-prenyl resulted only in a low level of co-IP. To exclude the influence of artificial protein aggregation, cells expressing only one type of protein (*i.e.*, either HA-Cdc42 or GFP-tagged DHHC5) were mixed prior to lysis and analyzed in parallel ("mix" samples). As shown in Figure 3*C*, both Cdc42 and DHHC5 can be detected by the corresponding antibody (visible in "input" fractions), but no co-IP was observed. This further verifies the specificity of interaction between Cdc42 and DHHC5. Even with the usage of mixed lysates from cells after single transfection represents a reasonable negative control for interaction specificity (16, 17); we cannot completely exclude the possibility that noninteraction between DHHC5 and Cdc42-palm in mixed lysates reflects the fact that DHHC5 and Cdc42-palm only co-IP when both are colocalized at the plasma membrane.

DHHC5 facilitates Cdc42-mediated gene transcription

It has been shown that Cdc42 is involved in the regulation of gene transcription by activating serum response factor (SRF)–mediated transcription by the serum response element (SRE) (18). In our previous study, we demonstrated that Cys188 is necessary to induce SRE activation, whereas palmitoylation of Cys189 seems to be responsible for the fine-tuning of SRE activity (10). To monitor the role of DHHC5 in Cdc42-mediated SRF activation, neuroblastoma N1E-115 cells were transiently transfected with different Cdc42 constructs along with an SRE-driven luciferase reporter plasmid and a cytomegalovirus-driven expression control reporter (Fig. 4*A*) in the presence of either scrambled shRNA (control) or shRNA against DHHC5. In line with our previous observations, expression of Cdc42 WT and Cys189 mutant led to increased SRE activation, while mutation of Cys188, either alone or in combination with Cys189, resulted in reduced Cdc42-mediated SRE activation (Fig. 4*B*). Knocking down endogenous DHHC5 by a specific shRNA caused a strong decrease in activating SRF-mediated gene transcription in case of Cdc42 WT (1.0 ± 0.49 scrambled shRNA *versus* 0.29 ± 0.17 anti-DHHC5 shRNA) and C189A mutant (0.67 ± 0.25 scrambled shRNA *versus* 0.32 ± 0.20 anti-DHHC5 shRNA; Fig. 4*B*). The C188A mutant as well as the C188/189A double mutant did not show any difference in their ability to induce SRF-mediated gene expression in the presence or absence of DHHC5 (Fig. 4*B*). In addition, Cdc42-prenyl was used as a negative control. Here, we found that while Cdc42-prenyl was also able to induce SRF-mediated gene transcription, this activity was not modulated by knockdown of the endogenous DHHC5 (0.72 ± 0.16 scrambled shRNA *versus* 0.84 ± 0.15 anti-DHHC5 shRNA; Fig. 4*B*).

DHHC5-mediated Cdc42 palmitoylation maintains formation of dendritic spines in hippocampal neurons

We next investigated the functional role of DHHC5-mediated Cdc42 palmitoylation in respect to the regulation of dendritic morphology. Immunofluorescence analysis with specific anti-DHHC5 antibody revealed that DHHC5 was clearly detected in dendrites, being frequently localized within dendritic shafts (Fig. 5*A*). To modulate expression of endogenous Cdc42 and DHHC5, we generated adeno-associated virus (AAV) vectors encoding shRNA to silence Cdc42 or DHHC5, respectively. We also applied the bicistronic AAV construct (Fig. S2*E*) encoding shRNA against endogenous Cdc42 along with shRNA-resistant WT or C188/189A Cdc42-palm mutant.

Similar to results obtained after the silencing endogenous Cdc42, specific and verified knockdown of DHHC5 (Fig. S2, *F* and *G*) significantly decreased the number of dendritic spines compared with the control neurons expressing scrambled shRNA (Fig. 5, *B* and *C*). The spine density was 0.74 ± 0.16 μm^{-1} in control compared with 0.63 ± 0.11 μm^{-1} after Cdc42 knockdown (n = 17 (control), n = 19 (shCdc42), p = 0.038) and 0.57 ± 0.13 μm^{-1} after DHHC5 knockdown (n = 19, p = 0.001), demonstrating the importance of DHHC5 for the spine formation. When endogenous Cdc42 was replaced by shRNA-resistant WT Cdc42-palm isoform, formation of dendritic spines was rescued. In contrast, replacement of endogenous Cdc42 by its palmitoylation-deficient mutant

neuroblastoma N1E-115 cells with scr shRNA, shRNA against DHHC5, and HA-tagged DHHC5 (*left panel*) and scr shRNA, shRNA against DHHC5 or DHHC6, respectively (*right panel*). Upper panel shows palmitoylation of GFP-Cdc42 detected with anti-GFP antibody. *Lower panel* shows expression of GFP-Cdc42 detected with anti-GFP antibody as well. *E*, quantitative analysis of the palmitoylation of Cdc42-palm. The results are mean ± SD from five independent experiments. One-way ANOVA with Dunnetts' multiple comparison, *$p < 0.05$. *F*, neuroblastoma N1E-115 cells expressing HA-tagged Cdc42 either alone or together with DHHC5 were processed for APEGS assay followed by SDS-PAGE and Western blot with anti-HA antibody. PEG-2k = PEG maleimide to provide 2 kDa shift, NH_2OH = hydroxylamine treatment; post-NEM after exposing free thiols by hydroxylamine (used as a negative control). G, stoichiometry of endogenous Cdc42 was analyzed using APEGS assay in primary cultures of rat hippocampal neurons. Representative Western blot with anti-Cdc42 antibody is shown. PEG-2k = PEG maleimide 2 kDa, NH_2OH = hydroxylamine treatment; post-NEM after exposing free thiols by hydroxylamine (used as a negative control). APEGS, acyl-PEGyl exchange gel shift; HA, hemagglutinin; qRT-PCR, quantitative RT-PCR.

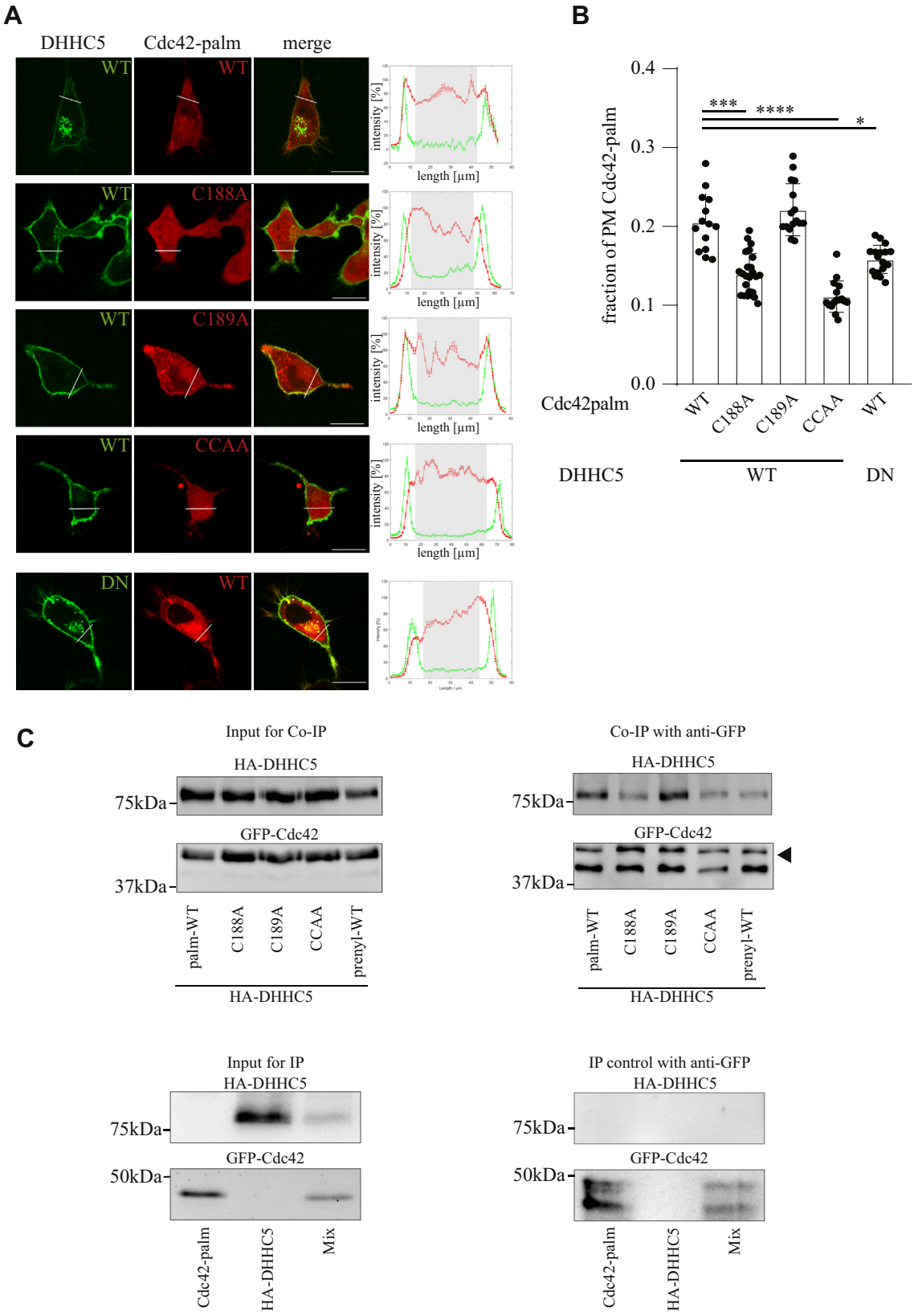

Figure 3. Interaction between DHHC5 and Cdc42 in neuroblastoma cells. *A*, N1E-115 cells were transfected with GFP-tagged DHHC5 WT or its dominant negative mutant (DN) together with mCherry-tagged Cdc42 WT or its cysteine mutants, as indicated. Subcellular distribution of recombinant proteins was analyzed in living cell by confocal microscopy. Representative images are shown. Corresponding fluorescence intensity profiles display localization of GFP-DHHC5 (*green*) and mCherry-Cdc42 (*red*) within individual cells. The scale bar represents 20 μm. *B*, quantification of the fluorescence intensity ratio for the coexpressed proteins. The plasma membrane region (assessed by DHHC5 channel) and the whole cell were selected for analyses as two different regions of interest (ROIs). The integrated density (area × mean intensity) was quantified in each ROI for mCherry-Cdc42 channel. After that, the fraction Cdc42-palm resided at the plasma membrane in comparison to whole cell Cdc42-palm intensity was calculated; $^{*}p < 0.05$,< $^{****}p < 0.0001$, Kruskal–Wallis test with

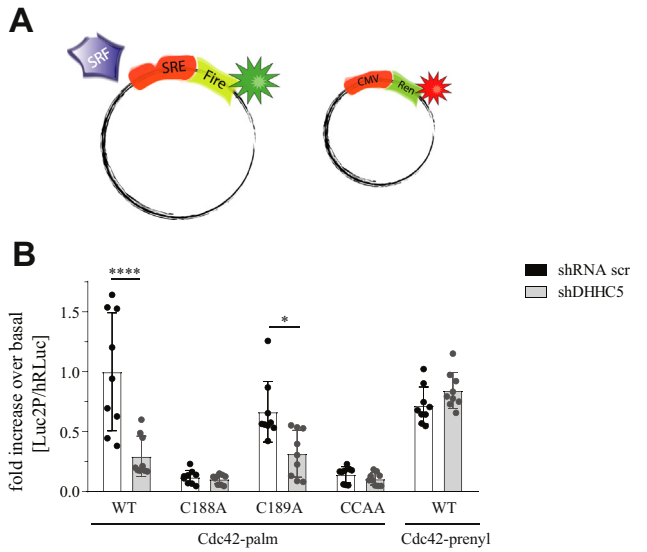

Figure 4. Functional impact of DHHC5-mediated Cdc42 palmitoylation of gene transcription. *A*, schematic representation of dual-luciferase reporter assay. *B*, neuroblastoma N1E-115 cells were transiently transfected with constructs indicated along with the SRE-driven luciferase reporter construct as well as CMV-driven reporter construct. Luciferase activity was measured 16 h post-transfection. The results are shown as mean ± SD from nine experiments. *$p < 0.01$; ****$p < 0.0001$; two-way ANOVA with Bonferroni's multiple comparison test. CMV, cytomegalovirus promotor; Fire, Firefly luciferase; Ren, Renilla luciferase, SRE, serum response element; SRF, serum response factor.

C188/189A resulted in significantly reduced number of dendritic spines compared with the neurons expressing Cdc42 palm WT (Cdc42-palm rescue 0.63 ± 0.12 μm^{-1}; C188/189A mutant rescue 0.52 ± 0.12 μm^{-1}; $p = 0.028$ Fig. 5, *B* and *C*). Because in these experiments the expression of endogenous DHHC5 was not affected, we assume that differences in spine density obtained upon Cdc42 rescue arose from DHHC5-mediated Cdc42 palmitoylation.

Finally, we addressed the question about the possible role of DHHC5-mediated Cdc42 palmitoylation during development. To this end, we determined the expression profile for both Cdc42 and DHHC5 in the mouse hippocampus at different stages of postnatal development using quantitative RT-PCR. This approach revealed that DHHC5 transcripts were upregulated during development, while the expression levels of the Cdc42 mRNA transcripts were not modulated (Fig. 5*D*). Since the protein expression level is assumed to roughly correlate with the level of mRNA transcripts, these data suggest that expression of DHHC5 protein undergoes developmental regulation. Such differences in the expression levels might result in profound changes of the enzyme:substrate ratio (*i.e.*, DHHC5:Cdc42) from 0.8:1 at P2, to 2.4:1 at P21, and 2.3:1 at P90, leading to increasing efficiency of Cdc42 palmitoylation by DHHC5.

Discussion

In this study, we underpinned the importance of Cdc42 palmitoylation in respect to its neuronal functions and identified DHHC5 as a prominent Cdc42 PAT driving its palmitoylation in neuroblastoma cells and hippocampal neurons. In addition to DHHC5, we identified DHHC10 and DHHC17, which could also increase palmitoylation of Cdc42. These three DHHCs have different intracellular distribution with DHHC5 being the only PAT residing at the plasma membrane (13). This is particularly important since the functional role of Cdc42 has typically been attributed to its function at the plasma membrane. In neurons, DHHC5 was also found to traffic through the vesicular system toward the synaptic spines, where it can regulate both, localization and assembly of synaptic proteins (19). In contrast, DHHC10 and DHHC17, which belong to the different PAT subfamilies, mainly reside within the Golgi and endoplasmic reticulum compartments (14). Because DHHC5 is known to be critically involved in spine formation (12, 13) and because it is highly abundant in the hippocampus (20, 21), we focused on the characterization of this PAT.

There is no general consensus sequence for palmitoylation, and enzyme-substrate recognition mechanisms are still under investigation. In case of DHHC5, it has been shown that it might interact with its substrate phospholemman (PLM) *via* 120 amino acid region of the DHHC5 carboxyl terminus close to the transmembrane domain, while the DHHC5 PDZ-binding motif was not involved (22). A more recent study revealed that it is rather the direct interaction of DHHC5 with the alpha-subunit of the sodium pump, which is not a DHHC5 substrate by itself, that triggers the formation of interaction complex with PLM (23). In contrast, binding and palmitoylation of the neuronal protein glutamate receptor interacting protein (GRIP1b) require the PDZ-binding motif within DHHC5 (24). This motif in also involved in interaction of DHHC5 with the synaptic scaffold protein PSD-95 (13). Our data also revealed a possible interaction between DHHC5 and Cdc42. However, the molecular mechanisms of Cdc42 recognition by DHHC5 were not elucidated in detail and should thus be addressed in future studies to rule out the direct or indirect (*via* adapter proteins) nature of this enzyme–substrate interaction. One intrigue possibility could be the activation of DHHC5 *via* its palmitoylation. Indeed, previous proteomic studies revealed that DHHC5 could be palmitoylated at its C-terminal cysteine residue localized abroad of DHHC catalytic core (25). It was also proposed that palmitoylation of DHHC5 causes conformational changes to allow substrate selection, as it has been shown for interaction with DHHC5 substrate Golga7b (15). One recent study showed that DHHC20 can palmitoylate DHHC5 at its C terminus and thus

Dunn's multiple comparison test. *C*, N1E-115 cells were cotransfected with HA-tagged DHHC5 and indicated GFP-tagged Cdc42, followed by immunoprecipitation (IP) with an anti-GFP antibody and Western blot with anti-HA antibody. As a control, mixed lysates from the single transfected cells (mix) were applied to IP. *Left*: input (expression) for the immunoprecipitation, *top*: DHHC5 detected with anti-HA antibody. *Second panel*: expression of Cdc42 variants and corresponding mutants detected with anti-GFP antibody. Similar order in the single transfections below on the *left*. *Right*: proteins detected after IP(co-IP) with anti-GFP antibody. *Top panel*: immunoprecipitated HA-tagged DHHC5 visualized with anti-HA antibody. *Second panel*: Cdc42 variants detected with anti-GFP antibody. Similar order in the single transfections below on the *right*. Representative Western blots are shown (N = 3). co-IP, coimmunoprecipitation; HA, hemagglutinin.

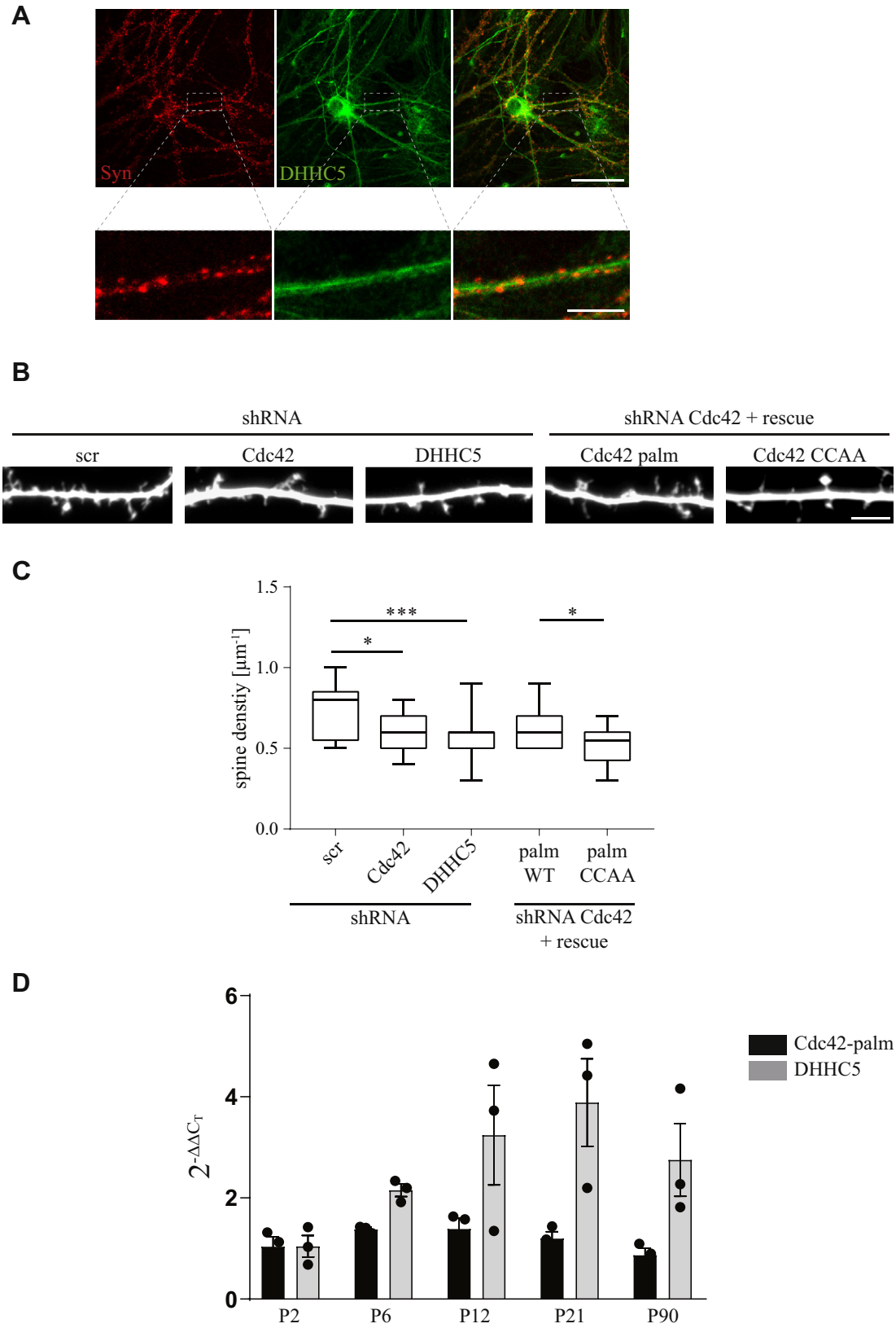

Figure 5. DHHC5-mediated Cdc42 palmitoylation modulates spinogenesis. *A*, primary cultures of mouse hippocampal neurons were fixed at DIV14 and stained with antibody against synaptophysin (Syn) and DHHC5 followed by confocal microscopy. Representative image is shown. The scale bar represents 50 µm. Scale bar inset: 10 µm. *B*, representative images showing dendritic morphology of hippocampal neurons infected with different AAV constructs as indicated. The scale bar represents 5 µm. *C*, the number of spines was calculated per micrometer of dendrite. The results are represented as min-to-max box-whiskers from at least three independent experiments. *$p < 0.05$; ***$p < 0.001$, one-way ANOVA with Sidak's multiple comparison test. *D*, relative expression ratios between Cdc42 and DHHC5 in the mouse hippocampus were determined at different stages of postnatal development using real-time PCR. AAV, adeno-associated virus; DIV, day *in vitro*.

regulates its ability to interact with the cardiac sodium pump, in this way creating the recognition and binding site for its substrate PLM (23). We have previously reported a reduced palmitoylation of Cdc42 in a mouse model of 22q11.2 deletion syndrome with DHHC8 belonging to the deleted genes (11). On the other hand, overexpression of DHHC8 in neuroblastoma N1E-115 cells did not result in increased Cdc42 palmitoylation, suggesting that DHHC8 can regulate Cdc42 palmitoylation being a PAT for DHHC5. Alternatively, DHHC8 can directly palmitoylate Cdc42 in a cell-type dependent manner. It has been shown that DHHC5 and DHHC8 are highly related and can share their substrates (19, 26). For example, both enzymes are reported to palmitoylate Grip1 as well as ankyrin-G (24, 27). In case of ankyrin-G, neither the single KO of DHHC5 nor DHHC8 reduced the palmitoylation level of ankyrin-G, while the double KO led to reduced ankyrin-G palmitoylation in MDCK cells (27).

In addition, protein palmitoylation could be hierarchically organized in time and space (28). Spatially, Golgi-resided DHHC17 or DHHC8 or even other PATs might be important for initial palmitoylation of Cdc42 immediately after synthesis. This will avoid a stable prenylation of Cdc42-palm and allow for the targeted transport of Cdc42 to dendrites and its insertion into the plasma membrane, where it could be a substrate for repeated palmitoylation by DHHC5. Our data show that the expression level of DHHC5 is increasing during development, while expression of Cdc42 was not affected. An age-dependent expression of DHHC5 was also reported for cultured neurons (24). The increasing ratio of DHHC5 to Cdc42 will result in more efficient Cdc42 palmitoylation within dendritic spines, which in turn will boost spinogenesis and spine maturation. Moreover, DHHC5 activity can be modulated upon synaptic activity (13), providing additional mechanism for the fine-tuning of Cdc42 palmitoylation and, as consequence, its activity in dendrites. Supporting this view, we obtained that the relative low level of basal Cdc42 palmitoylation obtained in N1E-115 cells (8%) was doubled upon DHHC5 overexpression. Also in hippocampal neurons, Cdc42 palmitoylation under basal conditions was relatively low. Future studies will thus be needed to more precisely evaluate the structural requirements for DHHC5–Cdc42 interaction and DHHC5 activation.

Experimental procedures

Antibodies and reagents

A polyclonal rabbit GFP antibody (used in IP) was purchased from GeneTex and a polyclonal goat horseradish peroxidase (HRP)–conjugated GFP antibody was purchased from LifeSpan BioSciences (former Biozol). Goat HRP-conjugated biotin antibody was purchased from Sigma–Aldrich. Peroxidase-conjugated HA (HA= antibody (3F10) was purchased from Roche. A monoclonal Cdc42 antibody was purchased from BD Biosciences. A monoclonal mouse GAPDH antibody (6C5) was purchased from Merck Millipore. An anti-zDHHC5 chicken polyclonal antibody was purchased from Prosci. A polyclonal goat antisynaptophysin antibody (SYP C-20) was purchased from Santa Cruz Biotechnology.

Cell culturing and transfection

Murine neuroblastoma cells N1E-115 from American Type Culture Collection were grown and maintained in Dulbecco's modified Eagle's medium containing 10% of fetal bovine serum and 100 U penicillin/streptomycin at 37 °C and 5% CO_2. To analyze recombinant proteins, N1E-115 cells were transiently transfected with corresponding plasmids using Lipofectamine 2000 reagent according to the manufacturer's instruction.

Hippocampal neuron cultures were prepared from C57Bl/6J HanZtm mice at postnatal day 1 (P1) or Wistar rats according to an optimized protocol for hippocampal neurons (29).

Plasmids and mutagenesis

A brain-specific murine Cdc42 isoform (Cdc42-palm) was cloned into pcDNA3.1 (+) vector after fusion with a GFP to the N terminus. N-terminally HA-tagged Cdc42-palm was created by the insertion of Cdc42-palm sequence into BamHI restriction sites of pEF-BOS-HA vector. Cdc42 mutants, derived from pcDNA3.1 (+) GFP-Cdc42-palm, are described in detail elsewhere (10). mCherry-tagged Cdc42-palm construct was obtained by using overlap-extension PCR, in which GFP was replaced by mCherry. HA-tagged Cdc42-palm mutants were created by site-directed mutagenesis as reported in the aforementioned publication. DHHC proteins were encoded by pEF-BOS-HA vectors as obtained in (30).

Used shRNAs were obtained from Oligoengine and under control of H1 promoter in either pAAV, pSUPER.neo+GFP, or pSUPERIOR.neo+GFP vector. The following sequences were used: shDHHC5: 5′-ACCTCCACCTCCTATAAGA-3′; shRNA scramble: 5′-GCGCGCTTTGTAGGATTCG-3′, shRNA Cdc42: 5′-CTGTTTCCGAAATGCAGAC-3′. Furthermore, the following constructs were cloned in our lab and used: pAAV-shRNACdc42-rescueGFP-Cdc42palmWT, pAAV-shRNACdc42-rescueGFP-Cdc4palmCCAA, as well as pAAV-tdTomato.

Co-IP

Co-IP in N1E-115 cells that coexpressed GFP-tagged Cdc42 isoforms and HA-tagged DHHCs were performed using an antibody directed against GFP (1:250). Lysates were incubated with the antibody directed against GFP followed by incubation with Protein-A Sepharose, SDS-PAGE, and Western blotting either with a HRP-conjugated antibody against GFP (1:5000) or a HRP-conjugated antibody against HA (1:1000).

Click chemistry

To determine dynamic palmitoylation, click chemistry using the Click-IT system from Invitrogen according to the manufacturer's instruction was performed. Therefore, N1E-115 cells were transfected with GFP-tagged Cdc42-palm. 12 h after transfection; the cells were either incubated with 50 μM palmitic acid azide or just dimethyl sulfoxide for additional 4 h. After the cells got lysed, 200 μg of total protein were incubated with 40 μM biotin alkylene in the presence of 2 mM $CuSO_4$.

The cell lysates were further processed by methanol–chloroform precipitation. Additionally, cell lysates were immune-precipitated with polyclonal rabbit GFP antibody and protein A-Sepharose. After washing, the protein complex was eluted, purified by trichloroacetic acid-acetone precipitation, and lysates were subjected to SDS-PAGE and Western blotting. Former palmitoylated Cdc42-palm was detected using a HRP-conjugated Biotin antibody (1:500), whereas total Cdc42-palm was detected using a HRP-conjugated GFP antibody (1:1000).

Acyl-biotinyl exchange assay

N1E-115 cells transfected with GFP-tagged Cdc42 were lysed in buffer containing 10 mM N-ethylmaleimide (NEM), and proteins were precipitated with methanol–chloroform extraction. Cell lysates were divided into two portions. One portion was treated with 0.75 M hydroxylamine (pH 7.4) and the other portion with 37.5 mM Tris (pH 7.4), which was used as control. At the same time, proteins were labeled with N-[6-(Biotinamido)hexyl]-3′-(2′-pyridyldithio)-propionamide. Afterward, cell lysates were immune-precipitated with polyclonal rabbit GFP antibody and protein A-Sepharose. After washing, the protein complex was eluted and lysates were subjected to SDS-PAGE and Western blotting. Total Cdc42 was detected with HRP-conjugated GFP antibody, whereas palmitoylated Cdc42 was detected with HRP-conjugated biotin antibody. Images were taken by PeqLab FUSION SL and quantified with MATLAB.

APEGS assay

To investigate palmitoylation stoichiometry of Cdc42, we used the newly developed method APEGS (4, 31). N1E-115 cells transfected with HA-tagged Cdc42 were lysed in 4% SDS-lysis buffer (containing 5 mM EDTA and protease inhibitors PMSF and mix of chymostatin, leupeptin, antipain, pepstatin). Free thiol groups were blocked using 40 mM NEM. Tris(2-carboxyethyl)phosphine was added to reduce disulfide bonds at the initial blocking step of APEGS assay. Afterward, proteins were precipitated with methanol–chloroform extraction. After resuspending the pellets in 4% SDS buffer (5 mM EDTA in PBS), cell lysates were treated with 1.3 M hydroxylamine (NH_2OH) (pH 7.0). The control lysates were treated with 1.3 M Tris (pH 7.0). Sequentially, samples were precipitated and either incubated with 20 mM PEG methyl ether maleimide (2000 Da) or 20 mM NEM. Finally, lysates were subjected to SDS-PAGE and Western blotting. Cdc42 was detected with peroxidase-tagged HA antibody. Images were taken by PeqLab FUSION SL and quantified using MATLAB.

A similar protocol was used to investigate the palmitoylation status of endogenous Cdc42. Therefore, hippocampal cultures from E18 rats were used at DIV23. In the end, Cdc42 was detected by a monoclonal Cdc42 antibody.

Confocal imaging, line profiles, and morphometric analysis

N1E-115 cells were plated on 18 mm coverslips and transiently transfected with corresponding Cdc42 and DHHC5-encoding plasmids. After overnight incubation, cells were subjected to confocal imaging and z-stack acquisition using Zeiss LSM 780. Membrane/cellular profiles were carried out semimanually using self-written MATLAB script. The quantitative analyses were performed according to Gorinski *et al.* (17). In brief, using Fiji software (https://imagej.net/software/fiji/), the plasma membrane region (assessed by DHHC5 channel) and the whole cell were selected for analyses as two different regions of interest. The integrated density (area × mean Intensity) was quantified in each region of interest for mCherry-Cdc42 channel. After that, the fraction Cdc42-palm resided at the plasma membrane in comparison to whole cell Cdc42-palm intensity was calculated (Fig. 3*B*).

For morphometric analysis of hippocampal neurons, neuronal cultures were sparsely transfected with an AAV vector encoding cytosolic tdTomato together with one of the indicated pAAV constructs (pAAV-shRNA scramble, pAAV-shRNA Cdc42, pAAV-shRNA DHHC5, pAAV-shRNA Cdc42-rescue GFP-Cdc42palmWT, and pAAV-shRNA Cdc42-rescue GFP-Cdc4palmCCAA; Figs. 5*B* and S2*A*) at DIV7 and cultured for 7 days post-transfection. Imaging of hippocampal neurons was carried out with Zeiss LSM 780 at DIV14. Number of short dendritic protrusions (<4 μm) per 1 μm dendrite of hippocampal neurons were analyzed using a custom-written software SpineMagick (https://zenodo.org/record/6114928#.YpnwuqhBw-U) (patent no. PCT/EP2012/065515) in a blinded experimental fashion as described before (32).

Immunocytochemistry

Primary hippocampal neurons were stained on DIV17 with synaptophysin antibody (C-20) from Santa Cruz (sc-7568) and DHHC5 antibody from ProSci Incorporation (#54-211). For that, neurons were fixed and permeabilized with ice-cold methanol and blocked with normal donkey serum. As secondary antibodies, we applied donkey antigoat and donkey antichicken from Jackson ImmunoResearch Laboratories, Dianova.

Dual luciferase reporter assay

To measure the activation of gene expression controlled by SRF, we used a dual-luciferase reporter assay in a 96-well format, and the luminescence was quantified with a Mithras LB 940 system. The pGL4.34[luc2P/SRF-RE/Hygro] plasmid was used as reporter and pGL4.50[luc2/CMV/Hygro] was used as control. Both plasmids were cotransfected in N1E-115 cells together with indicated Cdc42 isoforms or mutants. Cells were analyzed 16 h after transfection as described before (33, 34).

Quantitative real-time PCR

To analyze the expression level of Cdc42 and DHHC5 and DHHC10, total RNA was isolated from hippocampi of mice using TRIzol followed by complementary DNA synthesis using SuperScript III First-Strand Synthesis System according to the manufacturer's instructions. Primers (6-carboxyfluorescein and 6-carboxytetramethylrhodamine labels) were ordered as

TaqMan Gene Expression probes (Cdc42-palm: for details see (10); DHHC5: Mm00523158_m1). Amplification reaction has been carried using StepOne Plus (Applied BioSystems), and data were analyzed and relatively compared using ΔΔCT method.

Statistical analysis

For statistical analysis, GraphPad Prism 7.0 software (GraphPad Software, Inc) was used. Results are expressed as mean ± SEM and mean ± SD. If not differently indicated, multiple comparisons were carried out using one-way or two-way ANOVA. The significance level was chosen as $p = 0.05$.

Data availability

The data that support the findings of this study are available from the corresponding author upon reasonable request.

Supporting information—This article contains supporting information.

Author contributions—A. W. and E. P. conceptualization; A. W., N. G., N. Y., and M. F. methodology; A. W. validation; A. W., J. L., Y. S., N. G., N. Y., M. F., and E. P. formal analysis; A. W., J. L., D. A. G., T. B., Y. S., S. S., N. G., N. Y., and M. F. investigation; A. W. writing–original draft; J. L., Y. S., N. G., N. Y., M. F., and E. P. writing–review & editing; A. W., J. L., Y. S., N. G., N. Y., and M. F. visualization; E. P. supervision; E. P. project administration; E. P. funding acquisition.

Funding and additional information—This work was supported by the DFG Grant PO732 to E. P. and grant LA4465 to J. L.

Conflict of interest—E. P. has equity interest in TLL The Longevity Labs. The authors declare that they have no conflicts of interest with the contents of this article.

Abbreviations—The abbreviations used are: AAV, adeno-associated virus; APEGS, acyl-PEGyl exchange gel shift; co-IP, coimmunoprecipitation; DIV, day *in vitro*; HA, hemagglutinin; HRP, horseradish peroxidase; PAT, palmitoyl acyltransferase; pcDNA, plasmid cloning DNA; PLM, phospholemman; SRE, serum response element; SRF, serum response factor.

References

1. Blaskovic, S., Blanc, M., and van der Goot, F. G. (2013) What does S-palmitoylation do to membrane proteins? *FEBS J.* **280**, 2766–2774
2. Tian, L., McClafferty, H., Jeffries, O., and Shipston, M. J. (2010) Multiple palmitoyltransferases are required for palmitoylation-dependent regulation of large conductance calcium- and voltage-activated potassium channels. *J. Biol. Chem.* **285**, 23954–23962
3. Fukata, Y., Dimitrov, A., Boncompain, G., Vielemeyer, O., Perez, F., and Fukata, M. (2013) Local palmitoylation cycles define activity-regulated postsynaptic subdomains. *J. Cell Biol.* **202**, 145–161
4. Yokoi, N., Fukata, Y., Sekiya, A., Murakami, T., Kobayashi, K., and Fukata, M. (2016) Identification of PSD-95 depalmitoylating enzymes. *J. Neurosci.* **36**, 6431–6444
5. Rocks, O., Peyker, A., Kahms, M., Verveer, P. J., Koerner, C., Lumbierres, M., *et al.* (2005) An acylation cycle regulates localization and activity of palmitoylated Ras isoforms. *Science* **307**, 1746–1752
6. Yap, K., Xiao, Y., Friedman, B. A., Je, H. S., and Makeyev, E. V. (2016) Polarizing the neuron through sustained Co-expression of alternatively spliced isoforms. *Cell Rep.* **15**, 1316–1328
7. Lee, S. J., Zdradzinski, M. D., Sahoo, P. K., Kar, A. N., Patel, P., Kawaguchi, R., *et al.* (2021) Selective axonal translation of prenylated Cdc42 mRNA isoform supports axon growth. *J. Cell Sci.* **134**, jcs251967
8. Kang, R., Wan, J., Arstikaitis, P., Takahashi, H., Huang, K., Bailey, A. O., *et al.* (2008) Neural palmitoyl-proteomics reveals dynamic synaptic palmitoylation. *Nature* **456**, 904–909
9. Nishimura, A., and Linder, M. E. (2013) Identification of a novel prenyl and palmitoyl modification at the CaaX motif of Cdc42 that regulates RhoGDI binding. *Mol. Cell. Biol.* **33**, 1417–1429
10. Wirth, A., Chen-Wacker, C., Wu, Y.-W., Gorinski, N., Filippov, M. A., Pandey, G., *et al.* (2013) Dual lipidation of the brain-specific Cdc42 isoform regulates its functional properties. *Biochem. J.* **456**, 311–322
11. Moutin, E., Nikonenko, I., Stefanelli, T., Wirth, A., Ponimaskin, E., De Roo, M., *et al.* (2017) Palmitoylation of cdc42 promotes spine stabilization and rescues spine density deficit in a mouse model of 22q11.2 deletion syndrome. *Cereb. Cortex* **27**, 3618–3629
12. Brigidi, G. S., Sun, Y., Beccano-Kelly, D., Pitman, K., Mobasser, M., Borgland, S. L., *et al.* (2014) Palmitoylation of δ-catenin by DHHC5 mediates activity-induced synapse plasticity. *Nat. Neurosci.* **17**, 522–532
13. Brigidi, G. S., Santyr, B., Shimell, J., Jovellar, B., and Bamji, S. X. (2015) Activity-regulated trafficking of the palmitoyl-acyl transferase DHHC5. *Nat. Commun.* **6**, 8200
14. Ohno, Y., Kihara, A., Sano, T., and Igarashi, Y. (2006) Intracellular localization and tissue-specific distribution of human and yeast DHHC cysteine-rich domain-containing proteins. *Biochim. Biophys. Acta* **1761**, 474–483
15. Woodley, K. T., and Collins, M. O. (2019) S-acylated Golga7b stabilises DHHC5 at the plasma membrane to regulate cell adhesion. *EMBO Rep.* **20**, e47472
16. Westmeyer, G. G., Willem, M., Lichtenthaler, S. F., Lurman, G., Multhaup, G., Assfalg-Machleidt, I., *et al.* (2004) Dimerization of β-site β-amyloid precursor protein-cleaving enzyme. *J. Biol. Chem.* **279**, 53205–53212
17. Gorinski, N., Bijata, M., Prasad, S., Wirth, A., Abdel Galil, D., Zeug, A., *et al.* (2019) Attenuated palmitoylation of serotonin receptor 5-HT1A affects receptor function and contributes to depression-like behaviors. *Nat. Commun.* **10**, 392417
18. Hill, C. S., Wynne, J., and Treisman, R. (1995) The Rho family GTPases RhoA, Rac1, and CDC42Hs regulate transcriptional activation by SRF. *Cell* **81**, 1159–1170
19. Fukata, Y., Murakami, T., Yokoi, N., and Fukata, M. (2016) Local palmitoylation cycles and specialized membrane domain organization. *Curr. Top. Mem.* **77**, 97–141
20. Globa, A. K., and Bamji, S. X. (2017) Protein palmitoylation in the development and plasticity of neuronal connections. *Curr. Opin. Neurobiol.* **45**, 210–220
21. Shimell, J. J., Globa, A., Sepers, M. D., Wild, A. R., Matin, N., Raymond, L. A., *et al.* (2021) Regulation of hippocampal excitatory synapses by the Zdhhc5 palmitoyl acyltransferase. *J. Cell Sci.* **134**, jcs254276
22. Howie, J., Reilly, L., Fraser, N. J., Walker, J. M. V., Wypijewski, K. J., Ashford, M. L. J., *et al.* (2014) Substrate recognition by the cell surface palmitoyl transferase DHHC5. *Proc. Natl. Acad. Sci. U. S. A.* **111**, 17534–17539
23. Plain, F., Howie, J., Kennedy, J., Brown, E., Shattock, M. J., Fraser, N. J., *et al.* (2020) Control of protein palmitoylation by regulating substrate recruitment to a zDHHC-protein acyltransferase. *Commun. Biol.* **3**, 1–10
24. Thomas, G. M., Hayashi, T., Chiu, S.-L., Chen, C.-M., and Huganir, R. L. (2012) Palmitoylation by DHHC5/8 targets GRIP1 to dendritic endosomes to regulate AMPA-R trafficking. *Neuron* **73**, 482–496
25. Yang, W., Di Vizio, D., Kirchner, M., Steen, H., and Freeman, M. R. (2010) Proteome scale characterization of human S-acylated proteins in lipid raft-enriched and non-raft membranes. *Mol. Cell. Proteomics MCP.* **9**, 54–70
26. Fukata, Y., and Fukata, M. (2010) Protein palmitoylation in neuronal development and synaptic plasticity. *Nat. Rev. Neurosci.* **11**, 161–175

27. He, M., Abdi, K. M., and Bennett, V. (2014) Ankyrin-G palmitoylation and βII-spectrin binding to phosphoinositide lipids drive lateral membrane assembly. *J. Cell Biol.* **206**, 273–288
28. Abrami, L., Dallavilla, T., Sandoz, P. A., Demir, M., Kunz, B., Savoglidis, G., *et al.* (2017) Identification and dynamics of the human ZDHHC16-ZDHHC6 palmitoylation cascade. *eLife* **6**, e27826
29. Kobe, F., Guseva, D., Jensen, T. P., Wirth, A., Renner, U., Hess, D., *et al.* (2012) 5-HT 7 R/G 12 signaling regulates neuronal morphology and function in an age-dependent manner. *J. Neurosci.* **32**, 2915–2930
30. Fukata, M., Fukata, Y., Adesnik, H., Nicoll, R. A., and Bredt, D. S. (2004) Identification of PSD-95 palmitoylating enzymes. *Neuron* **44**, 987–996
31. Kanadome, T., Yokoi, N., Fukata, Y., and Fukata, M. (2019) Systematic screening of depalmitoylating enzymes and evaluation of their activities by the acyl-PEGyl exchange gel-shift (APEGS) assay. In: Linder, M. E., ed., *Methods in Molecular BiologyProtein Lipidation: Methods and Protocols*, Springer, New York, NY: 83–98. https://doi.org/10.1007/978-1-4939-9532-5_7
32. Bijata, M., Labus, J., Guseva, D., Stawarski, M., Butzlaff, M., Dzwonek, J., *et al.* (2017) Synaptic remodeling depends on signaling between serotonin receptors and the extracellular matrix. *Cell Rep.* **19**, 1767–1782
33. Wang, H., Chen, C., Song, X., Chen, J., Zhen, Y., Sun, K., *et al.* (2008) Mef2c is an essential regulatory element required for unique expression of the cardiac-specific CARK gene. *J. Cell. Mol. Med.* **12**, 304–315
34. Ponimaskin, E. G., Profirovic, J., Vaiskunaite, R., Richter, D. W., and Voyno-Yasenetskaya, T. a (2002) 5-Hydroxytryptamine 4(a) receptor is coupled to the Galpha subunit of heterotrimeric G13 protein. *J. Biol. Chem.* **277**, 20812–20819